Vol. 703: 31–46, 2023
https://doi.org/10.3354/meps14200

MARINE ECOLOGY PROGRESS SERIES
Mar Ecol Prog Ser

Published January 12

Species-specific monitoring of *Skeletonema* blooms in the coastal waters of Ariake Sound, Japan

Kazuhiro Yoshida[1], Hiroshi Ota[2], Takuya Iwanaga[2], Aiko Yoshitake[2], Takayuki Mine[2], Mana Omura[3], Kei Kimura[3,*]

[1]Graduate School of Agriculture, Saga University, 1 Honjo-machi, Saga, Saga 840-8502, Japan
[2]Saga Ariake Fisheries Research and Development Center, 2753-2, Nagata, Ashikari, Ogi, Saga 849-0313, Japan
[3]Faculty of Agriculture, Saga University, 1 Honjo-machi, Saga, Saga 840-8502, Japan

ABSTRACT: *Skeletonema* is a cosmopolitan diatom observed in coastal waters that forms extensive blooms, largely underpinning coastal ecosystems and fisheries. Recent revisions to the phylogeny of *Skeletonema* have shown multiple pseudocryptic species within the type species *S. costatum*. We developed a novel species-specific quantitative PCR (qPCR) method to track the annual dynamics of 7 *Skeletonema* species, including the pseudocryptic species, in the coastal waters of Ariake Sound, Japan. Fortnightly monitoring revealed that each *Skeletonema* species had different seasonality and occurrence patterns. The significant findings related to: (1) the species-specific ecological strategies and (2) the ecophysiology of the 5 pseudocryptic species assigned as *S. costatum* (sensu lato). Three *Skeletonema* species (*S. costatum* [sensu stricto], *S. menzelii*, and *S. tropicum*) formed blooms in summer, while the copy number of other species increased in winter (*S. ardens*, *S. dohrnii/marinoi*, *S. grevillei*, and *S. japonicum*). Bloom dynamics also differed among species, with either single intense bloom events or sustained moderate blooms. Summer species bloomed successively under the highly dynamic summer conditions (high freshwater input and anticyclonic tropical typhoons). By contrast, in winter, multi-species blooms were observed under conditions of low sea surface temperature and solar insolation. The single-peak species intensely bloomed during an ephemeral optimal time whereas others sustained their biomass in the pax between the intense blooms. Our *in situ* species-specific monitoring study connects *ex situ* physiology and *in situ* distributions, highlighting the diverse ecophysiology within this cosmopolitan diatom genus.

KEY WORDS: Diatoms · qPCR · Coastal blooms · Seasonal dynamics · Population ecology

1. INTRODUCTION

Marine phytoplankton accounts for ~50% of global primary production (Field et al. 1998, Behrenfeld et al. 2001). Diatoms are among the most productive phytoplankton groups; their primary production accounts for ~40% of total marine production (Nelson et al. 1995, Falkowski et al. 1998). Marine diatoms are highly diverse (>20 000 species estimated; Guiry 2012), and span tropical, temperate, and polar waters (McMinn et al. 2012, de Vargas et al. 2015, Malviya et al. 2016). In particular, neritic diatoms often form extensive blooms in coastal waters (Hallegraeff & Jeffrey 1993, D'Silva et al. 2012, Yoshida et al. 2018, 2020), controlling coastal ecosystems, coastal fisheries (Riley 1947, Cushing 1989, Tam et al. 2008), ecological functioning (Hasle & Syvertsen 1997, Richardson 1997, Anderson et al. 2000, Sarmiento & Gruber 2006, Paerl & Justić 2012), and benthic biomass (e.g. bivalves and mussels; Peterson 1999, Pernet et al. 2012, Lucas et al. 2016). As such, understanding the bloom dynamics of ner-

*Corresponding author: kimurak@cc.saga-u.ac.jp

itic diatoms is critical to manage coastal fisheries and aquaculture (Anderson et al. 2000, Imai et al. 2006, Diaz & Rosenberg 2008, Day et al. 2012).

Among neritic diatoms, the centric cosmopolitan diatom genus *Skeletonema* is the most widespread bloom-forming group in coastal environments; it has been observed in all coastal waters except for the Antarctic coast (Kooistra et al. 2008, Assmy et al. 2019). Indeed, coastal blooms of *Skeletonema* have been recorded since the 19th century (e.g. Murray 1897, Hasle 1973, Smayda 1973, Wilson et al. 2021). Due to their abundance in coastal waters, their ecology and physiology have been actively investigated, particularly for *S. costatum* (Cleve 1900, Kaeriyama et al. 2011, Guo et al. 2016, Ogura et al. 2018, Wang et al. 2020, Thangaraj & Sun 2021). However, recent rDNA and minute electron microscopic surveys have reported 8 pseudocryptic species within this type species (Medlin et al. 1991, Sarno et al. 2005, 2007, Zingone et al. 2005). It has been postulated that *S. costatum* (sensu lato) is physiologically plastic, having a global distribution (Hasle 1973, 1997, Paasche et al. 1975, see also Kooistra et al. 2008); however, the surprising taxonomical finding of the pseudocryptic species indicates rather that the high physiological plasticity of *S. costatum* (sensu lato) reflects the physiology of multiple *S. costatum*-like species. To clarify this point, Kooistra et al. (2008) investigated the global distribution of each *Skeletonema* species using extensive culture collections from coastal waters worldwide. Kaeriyama et al. (2011) examined the growth response to temperature and irradiance of multiple *Skeletonema* species/strains in the laboratory. Although their work was the first to provide insights into the physiology of 'new' *Skeletonema* species, their results indicated that multiple species have similar physiological features; nearly all species could grow at 15–25°C. Accordingly, understanding why physiologically similar species do not exhibit similar distributions is important. Although physical dispersion may somewhat affect distribution (McMinn et al. 1997, Barton et al. 2010), natural environmental gradients primarily control distribution and population dynamics (Sakshaug et al. 1997, Shikata et al. 2009, Bouman et al. 2018, Eriksen et al. 2018, Westwood et al. 2018, Mino et al. 2020). However, the manual enumeration of each *Skeletonema* species, by visualizing faint morphological differences through microscopy (Sarno et al. 2005, 2007), is not feasible particularly under dense bloom conditions (Tomas 1997, Elder & Elbrächter 2010). Therefore, in this study we developed a *Skeletonema* species-specific quantitative PCR (qPCR) method targeting the hypervariable 28S rRNA D1–D3 region (Orsini et al. 2002) to independently discuss the annual dynamics of each *Skeletonema* species *in situ*.

Surface-water monitoring was conducted every 2 wk in the coastal waters of Ariake Sound, Japan, between 2019 and 2020. Ariake Sound is a semi-closed, shallow (20 m depth on average) embayment located in western Japan (Fig. 1), with 4 major rivers flowing into the sound (Tsutsumi 2006, Orita et al. 2015). The region actively supports aquaculture of the rhodophyte *Neopyropia yezoensis* (Oohusa 1993, Kito & Kawamura 1999, Tsutsumi 2006), a raw material of seaweed (nori) papers for sushi. Ariake Sound is a suitable location to study *Skeletonema*, as year-round *Skeletonema* blooms have been observed (Ishizaka et al. 2006, Enjoji et al. 2019, Yamaguchi et al. 2019, Feng et al. 2020). In particular, winter blooms are extremely intense, damaging seaweed aquaculture farms (Tsutsumi 2006, Yamaguchi et al. 2019). Using samples collected every 2 wk, the abun-

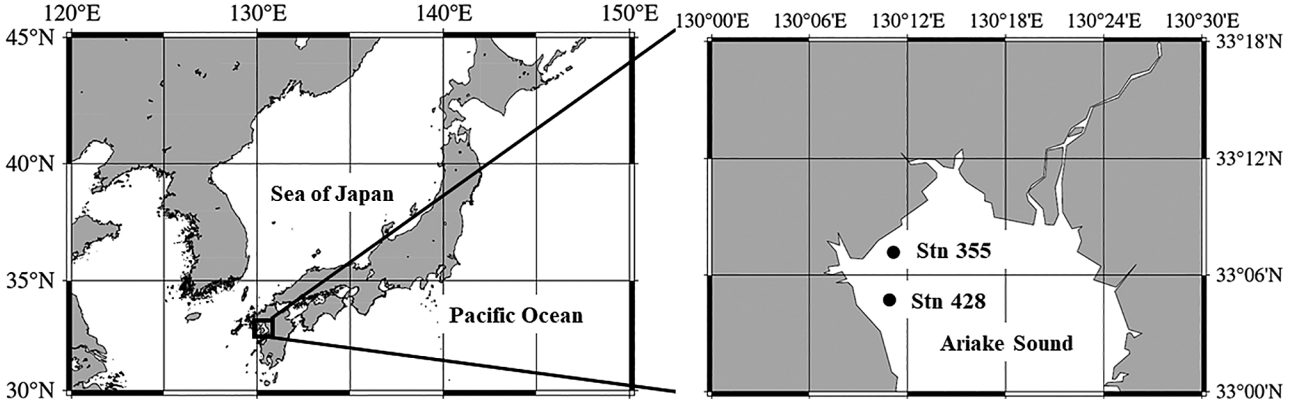

Fig. 1. Sampling stations in the coastal waters of Ariake Sound, Japan

dance of 7 *Skeletonema* species recorded in Ariake Sound (Yamada et al. 2014, Enjoji et al. 2019) was monitored with species-specific qPCR. In addition, correlation and multivariate analyses were carried out between species abundance and environmental variables to clarify species-specific annual dynamics. We aimed to develop *Skeletonema* species-specific qPCR techniques to monitor their dynamics in natural coastal waters such as those of Ariake Sound.

2. MATERIALS AND METHODS

2.1. Surface water sampling

Surface seawater sampling was conducted every 2 wk on spring tides at 2 stations (Stns 355 and 428 with 4.6 and 5.9 m bottom depth, respectively) in the coastal waters of Ariake Sound aboard RVs 'Kamome' and 'Chidori' from 4 June 2019 to 6 August 2020 (Fig. 1; Table S1 in the Supplement at www.int-res.com/articles/suppl/m703p031_supp.pdf); sampling was not conducted under extreme weather conditions (e.g. typhoons, damaging winds, high waves; Table S1). Surface seawater samples were collected from an approximately 0.5 m layer at high tide. Vertical temperature and salinity profiles were obtained using a conductivity-temperature-depth probe (RINKO-Profiler, ASTD102, JFE Advantech). Temperature and salinity (at 0.5 m) were recorded as sea surface temperature (SST) and sea surface salinity (SSS). Vertical water-column stability was quantified as the density difference between surface (0.5 m) and bottom depths, as per Sverdrup et al. (1942):

$$E' = 10^{-3}\,\Delta\sigma_t/\Delta z \quad (1)$$

where E' is the vertical stability of the water column, and $\Delta\sigma_t$ and Δz are the differences in σ_t and depth between 0.5 m and bottom depth, respectively. Nutrient concentrations (i.e. nitrate + nitrite, ammonium, phosphate, and silicate) were determined using an autoanalyzer (QuAAtro39, BL TEC K. K.) (Parsons et al. 1984, Hydes et al. 2010). The daily average sea surface photosynthetically available radiation (PAR, 400–700 nm; $PAR_{(0)}$) was recorded at the Saga Meteorological Observatory and was obtained from the Japan Meteorological Agency (https://www.jma.go.jp). The PAR diffuse attenuation coefficient, K_d(PAR), was estimated from Secchi-disk reading as per Poole & Atkins (1929):

$$K_d(\mathrm{PAR}) = 1.7/\text{Secchi-disk reading} \quad (2)$$

The resultant K_d(PAR) values were used to calculate the euphotic zone depth (Zeu) as 1% light depth referenced to surface incident light intensity (Kirk 2010).

2.2. Microscopy

Bright-field microscopy was performed to identify *Skeletonema* at the genus level and enumerate the corresponding diatom cells. It should be noted, however, that the solitary species *S. menzelii* could often be overlooked under light microscopy. After surface water sampling, unfixed seawater samples were immediately mounted on a 1 ml counting plate (S3600, Matsunami). Identification and enumeration of diatom cells at the genus level was conducted under a light microscope (4× oculars and 10× objective lenses, BX51, Olympus), based on Omura et al. (2012).

2.3. Species-specific qPCR targeting *Skeletonema* species

2.3.1. Unialgal cultures

Seven available unialgal cultures of *Skeletonema* species, including *S. ardens*, *S. costatum* (sensu stricto; hereafter *S. costatum*), *S. dohrnii*, *S. grevillei*, *S. japonicum*, *S. menzelii*, and *S. tropicum*, were obtained from the Microbial Culture Collection of the National Institute of Environmental Studies, Japan (Table 1). All species were maintained in modified SWM-3 medium enriched with 2 nM sodium selenite (Na_2SeO_3) (Imai et al. 1996) in artificial seawater (MARINE ART SF-1; Osaka Yakken) at 15°C and 100 µmol photons m^{-2} s^{-1} (white cool lamps). Then, 50 ml of each algal culture was filtered onto a 25 mm, 3 µm-pore omnipore polycarbonate filter (Merck). Cells retained on the filter were suspended in 200 µl of phosphate-buffered saline in a 1.5 ml tube (Ina Optika); DNA was extracted from the suspension using a Qiagen Blood & Tissue Kit. Briefly, 200 ml of the lysis buffer solution were added to the cell suspension and ultrasonicated for 1 min to disrupt algal cells. The solution was boiled at 100°C for 5 min to retrieve DNA from the filter. Both diatom debris and the filter were removed by pipetting and centrifugation; 200 ml of 100% ethanol (molecular biology grade, Wako) was then added to the clean solution. The mixture was applied to the spin column from the kit, and DNA extraction was carried out according to the manufacturer's instructions.

Table 1. Primer sets for *Skeletonema* species-specific quantitative PCR. The validity of each primer set was confirmed. See also Fig. S2 in the Supplement

Species	Strain ID	Forward (5′–3′)	Reverse (5′–3′)
Skeletonema ardens	NIES-2837	CGT TGA ATT GTG GTT TAT AGA AGC	CGA CCC AGG ATA TGA AAA GC
Skeletonema costatum	NIES-2838	CGT TCT TGC CTG GAA TCA	GGT AAA GAA AAC CAT TTC GAC AG
Skeletonema dohrnii	NIES-2839	CGT TCT TGC CTG GAA TCG	GGG GTA AAG AAA ACC ATT TTC TAA TT
Skeletonema grevillei	NIES-2840	GAA ACA AGT GTA AAG CGA CG	CGG GGT AAA TAA AAC AAT TTC CTC
Skeletonema japonicum	NIES-2841	CCG TTC TTG CCT GGA TTT G	CGA CCC AGG ATA TGA AAA GT
Skeletonema menzelii	NIES-2842	CCT GGG TTT GTT GTG CTT AA	ACC CAG AAC ATG AAG AGC A
Skeletonema tropicum	NIES-2537	CGA ATC TGG GTT AAG TGC A	CCG ACC CAG GAT ATG AAA AAT

2.3.2. Field samples

To monitor the bloom dynamics of the 7 *Skeletonema* species, we developed species-specific primer sets to discriminate among them. First, 50 ml of surface water samples was filtered onto a 25 mm, 3 µm pore omnipore polycarbonate filter (Merck). The DNA of the cells retained on the duplicated filters were extracted as described in Section 2.3.1.

2.3.3. Species-specific primer design

Species-specific qPCR targeting *Skeletonema* was carried out on the extracted DNA. Seven primer sets in the 28S rRNA gene, covering the D1–D3 hypervariable domain (Orsini et al. 2002), were designed to specifically amplify each *Skeletonema* species (Table 1). Primer validity was checked using the 7 corresponding unialgal cultures. DNA from unialgal cultures was extracted as described in Section 2.3.1. Further, unialgal DNA was amplified with the 7 primer sets to cross-check the specificity of each primer set.

2.3.4. qPCR standards

The copy numbers of each *Skeletonema* species were quantified to monitor the annual dynamics of each species, through qPCR standards. The target sequences of each species were amplified with each primer set, and the resultant PCR products were ligated into a linearized vector using a ligation kit (pGEM-T easy vector, Promega, WI, USA) following the manufacturer's protocol. The ligated vector was inserted into competent *Escherichia coli* cells (DH5α, Takara). After cloning, the extracted plasmids were digested with the restriction enzyme *Eco*RI (Nippon Gene) to obtain linearized qPCR standards. The DNA concentration of standards was converted to copy numbers, assuming an average molecular weight for DNA of 660 g mol^{-1}.

2.3.5. Quantitative PCR

Species-specific qPCR was undertaken with a qPCR thermal cycler (Mx3000, Stratagene), using a premixed qPCR reagent (Thunderbird SYBR qPCR mix, Toyobo) with species-specific primer sets. Triplicate samples were amplified by PCR using a series of diluted standards ($\times 10^{-2}$ to 10^{-8}); amplification curves were calibrated using a reference dye (ROX dye). The copy number of a sample was calculated from its amplification curve by interpolating the sample value into known standard values ($r^2 > 0.95$).

2.4. Statistical analysis

Pearson's correlation analysis was carried out using SigmaPlot ver. 11.0 (SysStat Software) to evaluate the relationships between variables assuming homoscedasticity. In addition, redundancy analysis (RDA) was performed to evaluate relationships between physicochemical properties and the copy numbers of each *Skeletonema* species as per Endo et al. (2018) and Yoshida et al. (2020). Detrended correspondence analysis was carried out beforehand to confirm the validity of the RDA analysis; the physicochemical and biological parameter gradients were sufficiently low (<3 standard deviations). Moreover, Hellinger transformation was conducted to normalize the copy number data (i.e. copy number) of the 7 *Skeletonema* species (Legendre & Gallagher 2001). Ordinations of environmental parameters and the copy number of *Skeletonema* species were plotted on an RDA coordinate plane. To describe the occurrence patterns of each *Skeletonema* species in a quantitative manner (discussed in Section 3.5), we defined the copy number of a species based on a 'sig-

nal vs. noise (S/N) ratio' approach with natural logarithms as follows: (1) calculating the total variance of the copy number of a species (P_n: noise); (2) rationing the copy number of each data point of a species (P_s: signal) as P_s/P_n (i.e. S/N ratio); and (3) defining the peak if its S/N ratio was $>10^{-16} \times P_s/P_n$, which was arbitrary in this study.

3. RESULTS

3.1. PCR specificity

The 7 species-specific primer sets successfully amplified each target species (Fig. S1); moreover, the amplification curves confirmed the specificity of the primer sets (Fig. S2). The specificity was validated through single peaks in the dissociation curves after qPCR runs (Fig. S3). A series of standards was properly amplified with the corresponding primer sets to establish a standard curve, which indicated that the qPCR protocols were accurately established. However, we hereafter defined *Skeletonema dohrnii* as *S. dohrnii*/*S. marinoi*, as these allied species could not be clearly discriminated with our primers (see Section 4.1).

3.2. Environmental variables

Dynamic seasonal variations were evident for SST and SSS, ranging from 10.5 to 30.3°C and 1.53 to 31.45 at Stn 355, and from 10.9 to 30.0°C and 2.42 to 31.82 at Stn 428, respectively. The highest and lowest SSTs were observed at both stations on 1 August 2019 and 10 February 2020, respectively (Fig. 2A,D; Table S1). During the summer, on 14 July 2020, extreme freshening of surface water to the lowest salinity was observed at both stations due to heavy rainfall on 6 July 2020 (209 mm d^{-1}; Japan Meteorological Agency recorded at the Saga Meteorological Observatory; https://www.jma.go.jp (Fig. 2A,D). Thus, significant negative relationships between SST and SSS were observed at both stations (Stn 355: $p = 0.013$; Stn 428: $p = 0.009$; Table 2). In general, the water column was well-mixed and relatively homogeneous in winter, having lower E' values, whereas steep density gradients with high E' values were observed in the summer (Fig. 2B,E). The euphotic zone depths (Zeu) ranged from approximately 1 to 4 m with marked variations, up to 6.5 m between August and September 2019 (Fig. 2C,D; Table S1). Both solar irradiance and Zeu, in general, were high in summer and low in winter (Fig. 2C,D; Table S1).

We also observed dynamic changes in nutrient concentrations throughout the sampling period. Nitrate and phosphate were sporadically depleted, while silicate concentrations were consistently high (Fig. 3; Table S1). Interestingly, the highest nutrient concentrations were observed only at Stn 428 after the extreme surface water freshening event on 14 July 2020 (Figs. 2D & 3). Nitrate and ammonium concentrations were negatively correlated with SSS at both stations ($p < 0.01$; Table 2). At Stn 355, nitrite and ammonium concentrations were independent of nitrate concentrations (e.g. the nitrite concentration exceeded that of nitrate concentration on 17 October 2019; Fig. 3A); however, nutrients were significantly and positively correlated with each other throughout the sampling period ($p < 0.05$, Table 2). Nitrate, ammonium, and silicate concentrations exhibited a positive relationship with vertical stability at both stations ($p < 0.05$, Table 2); similarly, phosphate concentrations were positively correlated with stability ($p = 0.002$, Table 2) at Stn 355 (Fig. 3A).

3.3. Diatom and total *Skeletonema* abundance as determined by light microscopy

Microscopic analysis revealed a wide range in the abundance of diatoms and the total *Skeletonema* (Fig. 4). At Stns 355 and 428, diatom abundance varied from 0 to 10 228 cells ml^{-1} and from 0 to 43 500 cells ml^{-1}, and that of total *Skeletonema* ranged from 0 to 10 200 cells ml^{-1} and from 0 to 30 900 cells ml^{-1}, respectively (Fig. 4; Table S1). We found significant correlations between total *Skeletonema* abundance and total diatom abundance at both stations ($p < 0.001$, Table 2) as well as between total diatom abundance and SSS at Stn 428 ($p = 0.012$, Table 2).

3.4. *Skeletonema* species-specific abundance (copies ml^{-1})

There were dynamic variations in copy number of the 7 target *Skeletonema* species throughout the sampling period (Fig. 5). The abundance, represented as copy number (copies ml^{-1}), ranged between 1 and 5 orders of magnitude throughout the sampling period (Fig. 5). Overall, the abundance variations were synchronized between the 2 sampling stations, although to different extents among species (Fig. 5). For instance, *S. ardens* blooms did

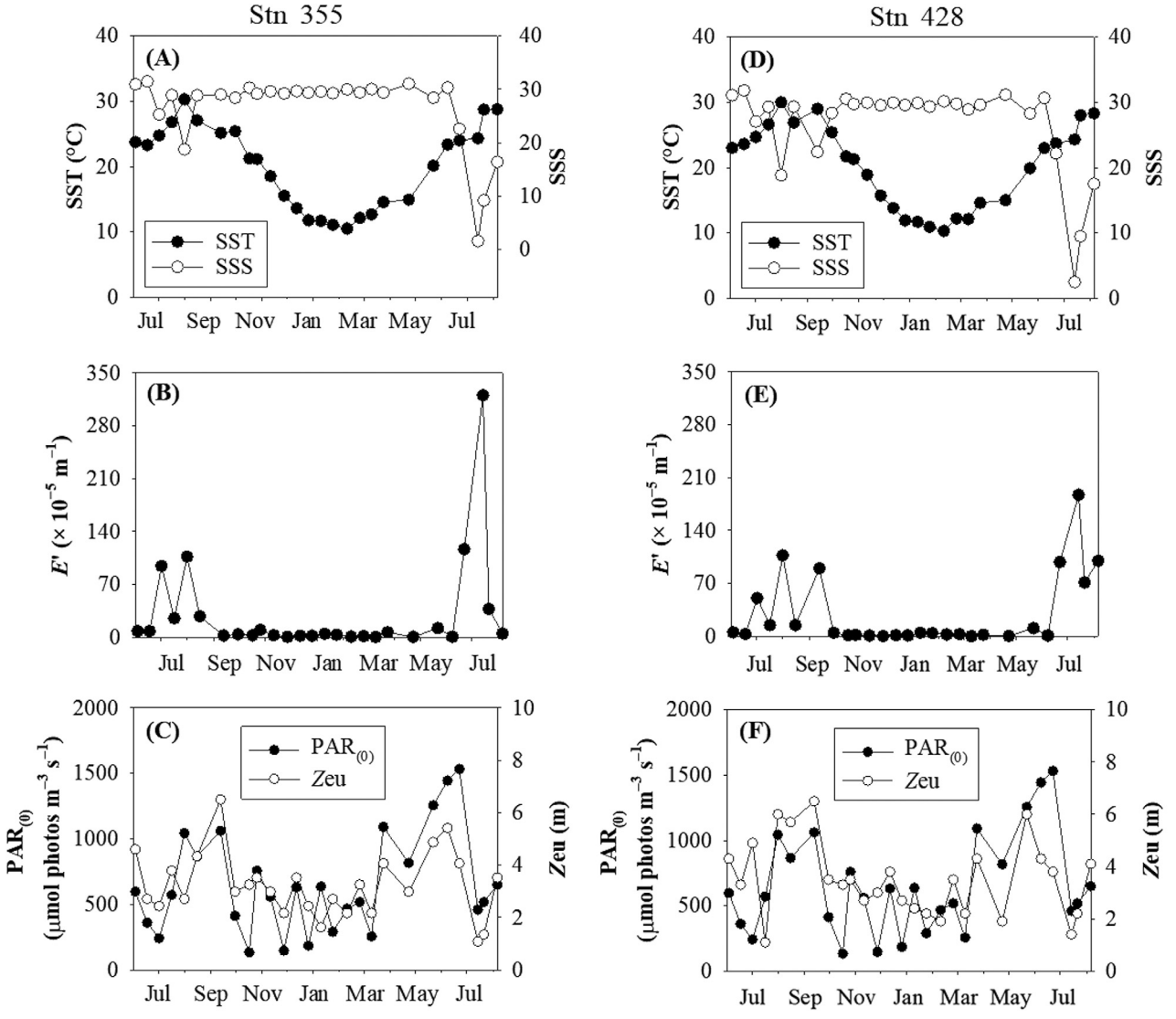

Fig. 2. Physical and optical properties in Ariake Sound in 2019/2020, Annual variations in: (A,D) sea surface temperature (SST) and salinity (SSS); (B,E) vertical water column stability (E'); and (C,F) solar insolation (photosynthetically available radiation, $PAR_{(0)}$) and euphotic zone depth (Zeu). Panels A–C and D–F show the physical and optical data at Stns 355 and 428, respectively

not concomitantly occur every time; however, the increases in November 2019 and January and March 2020 occurred concurrently at both stations (Fig. 5A); as such, synchronization between stations was more evident in *S. japonicum* (Fig. 5E).

3.5. Species-specific seasonality and occurrence patterns

In addition to the occurrence patterns, the 7 *Skeletonema* species showed seasonality; *S. ardens*, *S. dohrnii/marinoi*, *S. japonicum*, and *S. grevillei* increased in their copy number primarily in winter (Fig. 5A,C–E), while *S. costatum*, *S. menzelii*, and *S. tropicum* showed increased numbers in summer (Fig. 5B,F,G), although *S. tropicum* exhibited small increases in winter as well (Fig. 5G). Generally, the higher copy numbers of autumn/winter species often overlapped (i.e. co-occurrence of multiple species), whereas those of summer species were relatively independent (i.e. occurrence of a single species succeeded by another). No evident blooms were observed in spring in March and early winter in November (Fig. 5).

Similarly, the annual variation patterns differed among species: *S. ardens* showed multiple increases over a prolonged period from September 2019 to

Table 2. Correlations between environmental variables during the sampling period at: (A) Stn 355 and (B) Stn 428 in Ariake Sound, Japan. Pearson correlation coefficients (r) were calculated to assess the relationships between environmental variables, assuming homoscedasticity. **Bold** indicates significant relationships ($^{*}p < 0.05$, $^{**}p < 0.01$, $^{***}p < 0.001$). SST: sea surface temperature, SSS: sea surface salinity; NO_3, NO_2, NH_4, PO_4, and SiO_4: concentrations of nitrate, nitrite, ammonium, phosphate, and silicate, respectively; T*Skeletonema* and TDiatom: total cell abundance of *Skeletonema* and diatoms enumerated under bright-field light microscopy. $PAR_{(0)}$: averaged daily incident photosynthetically available radiation obtained from the Japanese Meteorological Agency; *Z*eu: euphotic zone depth as the 1% light depth referenced with surface light intensity calculated from the Secchi-disk reading, E': water-column vertical stability measured as a difference in density (σ_t) between 0.5 m and the bottom depth ($\Delta\sigma_t/\Delta z$)

(A) Stn 355	SSS	NO_3	NO_2	NH_4	PO_4	SiO_4	T*Skeletonema*	TDiatom	$PAR_{(0)}$	*Z*eu	E'
SST	**−0.485***	0.153	0.232	0.224	0.220	**0.627*****	−0.223	−0.012	0.294	0.254	0.356
SSS		**−0.525****	−0.274	**−0.641*****	−0.312	**−0.797*****	−0.142	−0.306	−0.023	**0.415***	**−0.789*****
NO_3			**0.461***	**0.792*****	**0.916*****	**0.725*****	−0.048	−0.153	−0.368	**−0.449***	0.688*****
NO_2				**0.464***	**0.500****	**0.424***	−0.019	−0.125	**−0.463***	−0.295	0.255
NH_4					**0.77*****	**0.713*****	−0.150	−0.126	−0.301	**−0.406***	**0.693*****
PO_4						0.606*****	−0.263	−0.315	−0.369	−0.269	0.560****
SiO_4							−0.097	−0.071	−0.001	−0.185	**0.751*****
T*Skeletonema*								**0.790*****	−0.068	**−0.481***	−0.063
TDiatom									−0.066	**−0.425***	−0.131
$PAR_{(0)}$										**0.650*****	0.076
*Z*eu											−0.334

(B) Stn 428	SSS	NO_3	NO_2	NH_4	PO_4	SiO_4	T*Skeletonema*	TDiatom	$PAR_{(0)}$	*Z*eu	E'
SST	**−0.491****	0.035	0.073	0.082	0.148	**0.66*****	−0.004	0.155	0.305	**0.437***	**0.575****
SSS		**−0.552****	−0.164	**−0.501****	−0.309	**−0.804*****	−0.377	**−0.474***	−0.077	0.075	**−0.913*****
NO_3			**0.543****	**0.769*****	**0.854*****	**0.512****	−0.051	−0.126	−0.277	−0.299	**0.507****
NO_2				**0.469***	**0.684*****	0.228	0.141	0.033	**−0.442***	−0.214	0.026
NH_4					**0.767*****	**0.472***	−0.107	−0.064	−0.266	−0.246	**0.468***
PO_4						**0.438***	−0.211	−0.212	−0.376	−0.294	0.280
SiO_4							0.247	0.289	0.133	0.024	**0.794*****
T*Skeletonema*								**0.854*****	−0.130	−0.327	0.066
TDiatom									−0.116	−0.256	0.195
$PAR_{(0)}$										**0.525****	0.221
Zeu											0.116

April 2020 (Fig. 5A), whereas *S. costatum* showed intense peaks in their copy numbers (i.e. 4 orders of magnitude) in August/September 2019 and in August 2020 (Fig. 5B). Similarly, *S. dohrnii/marinoi* and *S. tropicum* showed multiple peaks in copy number variations during winter–spring and summer–autumn transitions (Fig. 5C,G). In contrast, *S. grevillei*, *S. japonicum*, and *S. menzelii* showed a peak in their copy numbers (Fig. 5D–F); *S. menzelii* only exhibited a summer peak in 2020 at Stn 355 (Fig. 3F). Interestingly, the peak in copy number of *S. menzelii* was not entirely coupled with the total number of *Skeletonema* cells (Figs. 4 & 5F). In general, species which showed saw-toothed variations (1 to 2 orders of magnitude, except for the first increase in *S. tropicum*) did so over prolonged periods; in contrast, species with single peaks showed an increase in numbers occurring typically within 8 wk (Fig. 5)

3.6. Relationship between species abundance and environmental variables

The relationships between *Skeletonema* species abundance and environmental variables were generally similar, apart from some differences, between stations. *S. ardens* copy number was negatively correlated with $PAR_{(0)}$ at both stations ($p < 0.05$) and positively correlated with nitrite concentrations ($p = 0.006$, Table 3). The summer species *S. costatum* had positive and negative relationships with silicate concentrations and SSS, respectively, at Stn 428; no evident correlation was observed at Stn 355 (Table 3). The winter species *S. dohrnii/marinoi* was negatively correlated with SST at both stations and $PAR_{(0)}$ at Stn 355 ($p < 0.05$); however, the other winter species (i.e. *S. japonicum* and *S. grevillei*), did not show any conspicuous correlation with environmental variables (Table 3). At both stations, *S. menzelii* showed

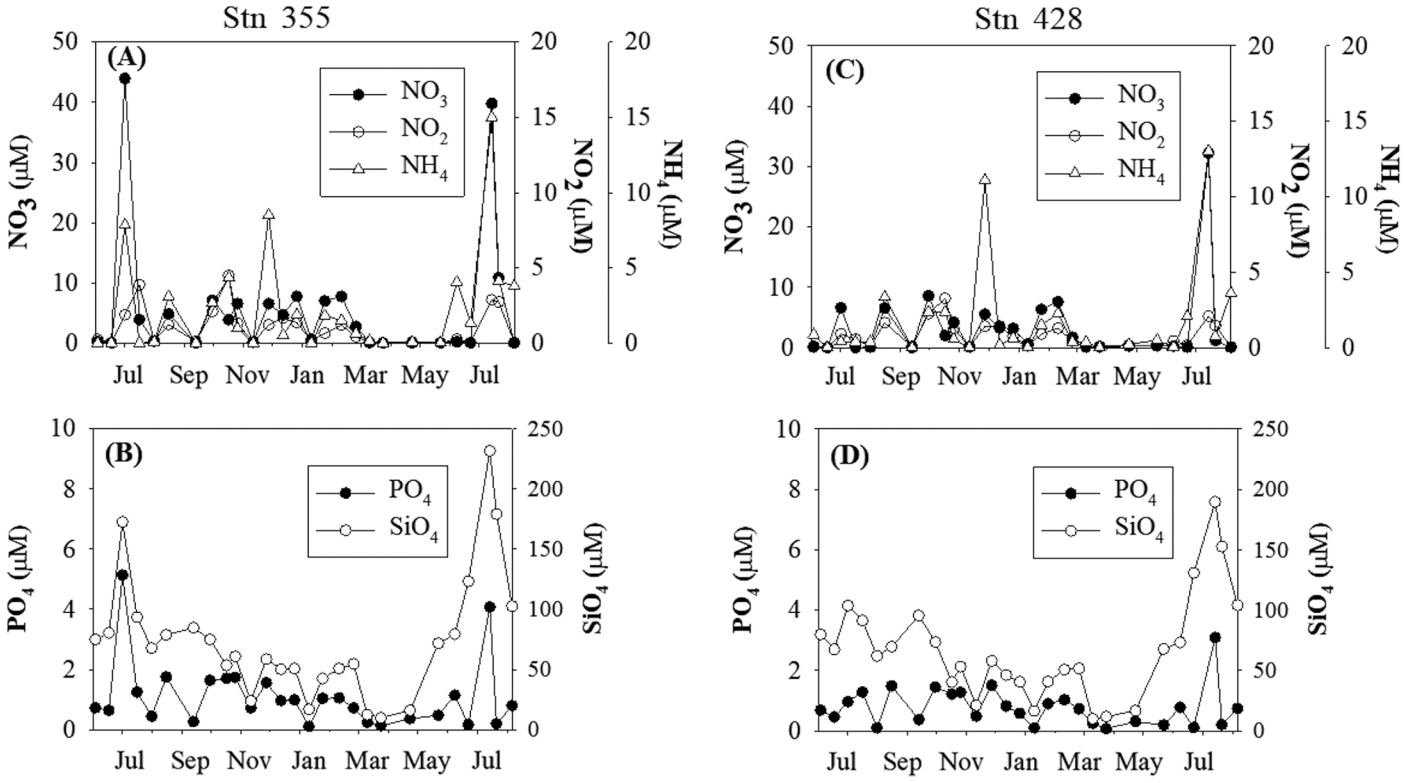

Fig. 3. Nutrient concentrations in surface water in the Ariake Sound in 2019/2020. Annual variations in: (A,C) nitrate (NO_3), nitrite (NO_2), and ammonium (NH_4); and (B,D) phosphate (PO_4) and silicate (SiO_4) concentrations. Panels A,B and C,D show the nutrient data at Stns 355 and 428, respectively

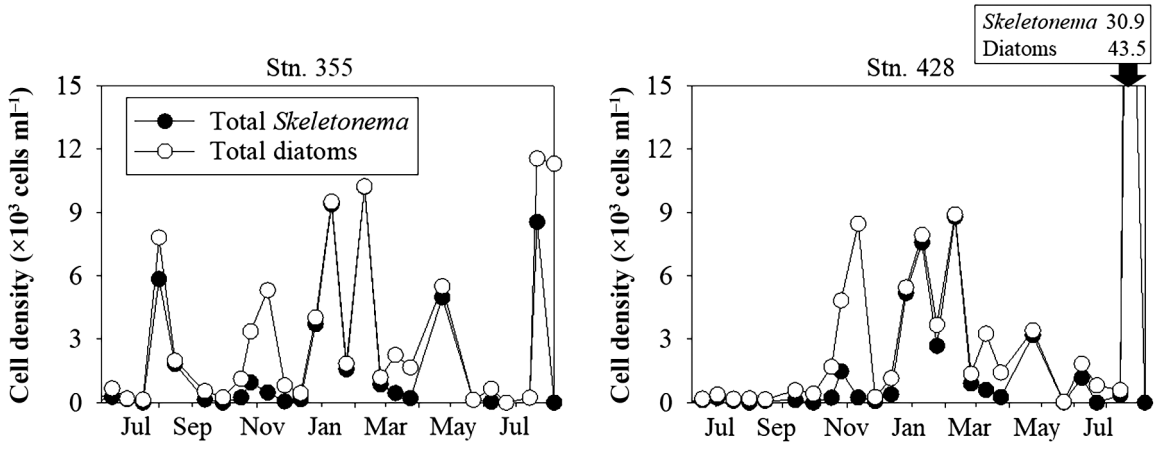

Fig. 4. Temporal variations in total *Skeletonema* and in total diatom cells as determined with bright field microscopy

significant positive relationships with $PAR_{(0)}$ ($p < 0.05$), while the copy number of *S. tropicum* was positively correlated with nitrite concentrations ($p < 0.01$, Table 3). Euphotic zone depth and vertical stability were not correlated with the abundance of any *Skeletonema* species (Table 3).

The RDA analysis produced similar results, with slight differences between stations; however, each axis showed small variances in both RDA panes for both stations (Fig. 6). In both RDA panels, the variance in the first axis may be largely attributed to the SST. Only *S. costatum* showed a significant positive score, while *S. dohrnii/marinoi, S. grevillei*, and *S. japonicum* showed evident negative scores on the first axis (Fig. 6). Other remarkable similarities were that the copy number of *S. ardens* was related to ammonium levels and *S. menzelii* followed similar directions to the vector of optical properties such as

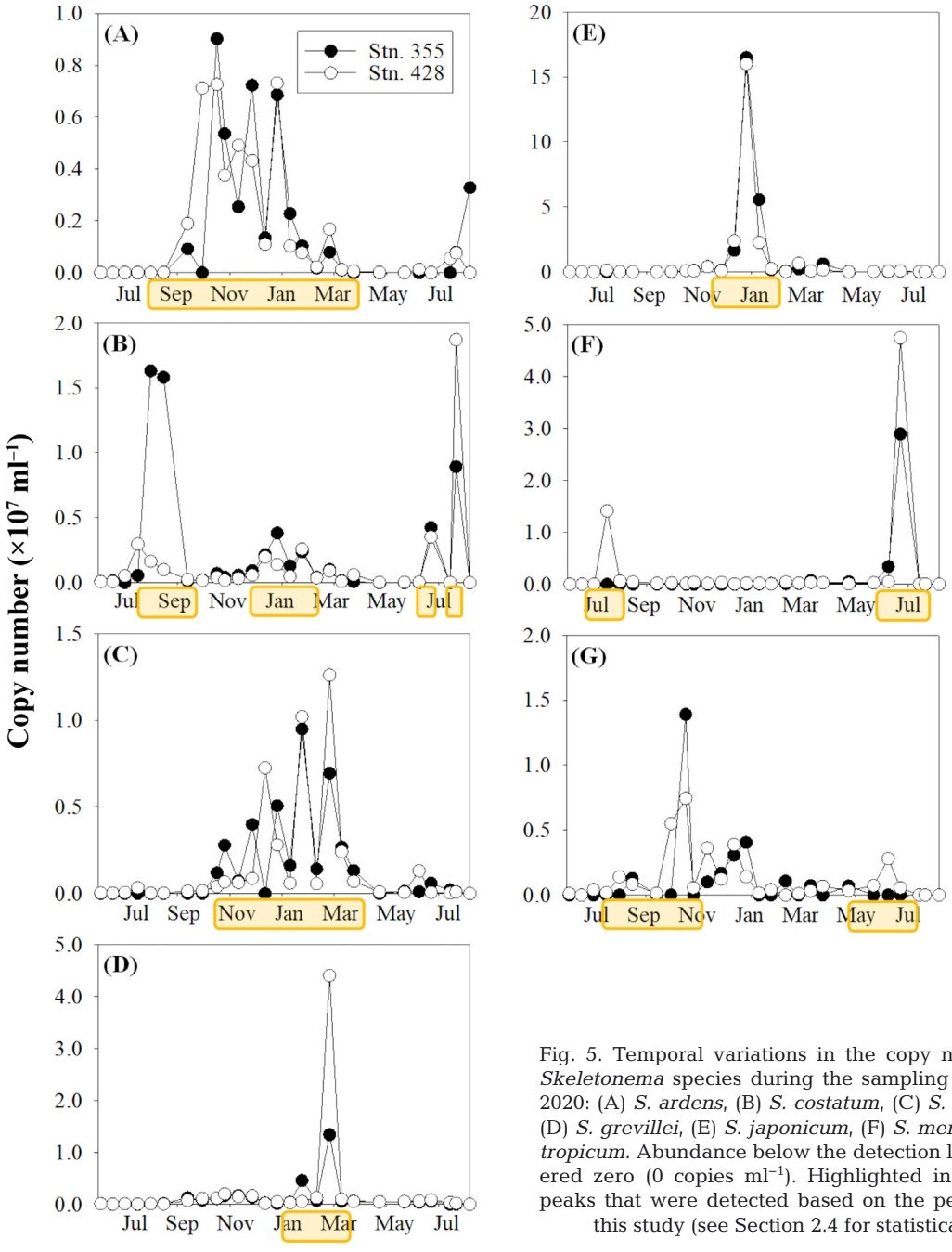

Fig. 5. Temporal variations in the copy numbers of each *Skeletonema* species during the sampling period in 2019/2020: (A) *S. ardens*, (B) *S. costatum*, (C) *S. dohrnii/marinoi*, (D) *S. grevillei*, (E) *S. japonicum*, (F) *S. menzelii*, and (G) *S. tropicum*. Abundance below the detection limit was considered zero (0 copies ml^{-1}). Highlighted in yellow are the peaks that were detected based on the peak definition in this study (see Section 2.4 for statistical analysis)

$PAR_{(0)}$ and *Z*eu (Fig. 6). Dominant variables on the second axis were optical properties and nutrient levels, although the scores of these variables in the panels were reversed (Fig. 6). Consistently, *S. menzelii* and *S. ardens* showed opposite vectors in the second axis with high scores (Fig. 6). Moreover, while *S. dohrnii/marinoi* and *S. tropicum* had relatively high positive scores in the panel of Stn 355 (Fig. 6A), other *Skeletonema* species had low scores (Fig. 6).

4. DISCUSSION

4.1. Primer specificity

This study is the first to track the *in situ* annual dynamics of 7 *Skeletonema* species, including 5 pseudocryptic species previously annotated as *S. costatum* (sensu lato), (i.e. *S. ardens*, *S. costatum* [sensu stricto], *S. dohrnii/marinoi*, *S. grevillei*, and *S. japonicum*), and 2 distinct species (*S. menzelii* and *S.*

Table 3. As in Table 2, but between the copy number of each *Skeletonema* species (copies μl^{-1}) and environmental variables during the sampling period at: (A) Stn 355 and (B) Stn 428 in Ariake Sound, Japan. SST: sea surface temperature, SSS: sea surface salinity; other abbreviations as in Table 2

	S. ardens	*S. costatum*	*S. dohrnii/marinoi*	*S. grevillei*	*S. japonicum*	*S. menzelii*	*S. tropicum*
(A) Stn 355							
SST	−0.207	0.377	**−0.637*** **	−0.378	−0.379	0.119	−0.130
SSS	0.141	−0.266	0.225	0.173	0.122	−0.091	0.182
NO_3	−0.065	−0.079	−0.045	−0.095	−0.009	−0.126	−0.047
NO_2	0.338	0.017	−0.093	−0.127	0.002	−0.186	**0.547****
NH_4	0.180	−0.053	−0.039	−0.125	−0.085	−0.052	0.106
PO_4	0.059	−0.115	−0.078	−0.090	−0.089	−0.173	0.088
SiO_4	−0.206	0.117	−0.320	−0.189	−0.187	0.177	−0.174
$PAR_{(0)}$	**−0.444***	0.197	**−0.383***	−0.124	−0.233	**0.509****	−0.365
*Z*eu	−0.165	−0.076	−0.234	0.013	−0.202	0.174	−0.053
E′	−0.242	0.165	−0.217	−0.166	−0.121	0.244	−0.152
(B) Stn 428							
SST	−0.100	0.226	**−0.552****	−0.267	−0.343	0.161	0.037
SSS	0.170	**−0.467***	0.216	0.106	0.123	−0.095	0.245
NO_3	0.054	−0.101	−0.013	−0.050	−0.024	−0.132	−0.030
NO_2	**0.513****	0.145	−0.003	−0.066	−0.016	−0.156	**0.588****
NH_4	0.131	−0.092	−0.138	−0.076	−0.107	−0.006	−0.034
PO_4	0.222	−0.200	−0.017	−0.008	−0.093	−0.159	0.153
SiO_4	−0.211	**0.413***	−0.263	−0.092	−0.185	0.314	−0.239
$PAR_{(0)}$	**−0.450***	−0.025	−0.218	−0.075	−0.247	**0.441***	−0.155
*Z*eu	−0.121	−0.211	−0.145	−0.006	−0.130	−0.050	0.059
E′	−0.245	0.193	−0.268	−0.127	−0.158	0.260	−0.272

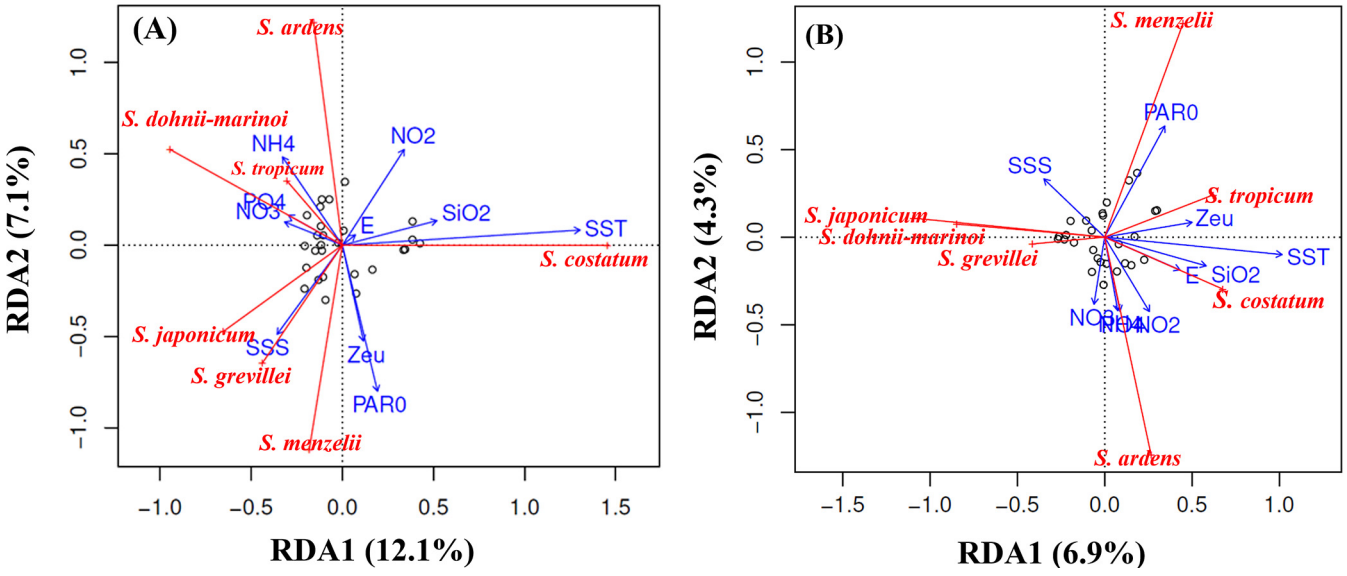

Fig. 6. Coordinate plane of the redundancy analysis (RDA) on the copy numbers of each *Skeletonema* species at: (A) Stn 355 and (B) Stn 428. The RDA was verified with detrended correspondence analysis that the lengths of gradients of environmental parameters were sufficiently small for RDA analysis (<3 SD). The contributions to the total variance (i.e. proportions explaining the total variance) are shown for each RDA axis; n = 27

tropicum) using our novel qPCR technique. This technique enables the quantification of pseudocryptic *Skeletonema* species that are difficult to identify with microscopy. In addition, the qPCR approach allows absolute quantification of each species in copy number ml^{-1}. This cannot be achieved through the widely used amplicon sequencing via high-throughput sequencing, which at best provides the relative

contributions of target organisms at the species level. We used the housekeeping 28S rRNA, recognized as a less variable gene compared with other markers (Rimet et al. 2019, Suzuki et al. 2000, Zhang et al. 2020, Pearson et al. 2021), even if our qPCR results might be biased by variations in copy number per cell among target species and bloom stages (Vasselon et al. 2018). Despite the limitations above, our qPCR technique is a powerful tool for the quantification of *Skeletonema* species in natural waters.

The 28S sequence of *S. dohrnii* was relatively similar to that of *S. marinoi*, and although to date *S. marinoi* has not been observed in Ariake Sound, Yamada et al. (2013, 2014) and Shevchenko & Ponomareva (2015) recorded *S. marinoi* in other Japanese waters. We used an *S. dohrnii* strain; however, these allied species might not be firmly discriminated with our primers, so here we defined *S. dohrnii* as *S. dohrnii*/*S. marinoi* (described in Section 3.1). Moreover, the annual dynamics of *S. menzelii* were inconsistent between our qPCR and microscopic *Skeletonema* evaluations (Figs. 4 & 5F). We may have missed this solitary species, which is difficult to identify under light microscopy. Although our qPCR technique successfully quantified this species, its cell abundance should be validated by electron microscopy.

This species-specific molecular survey provided novel and significant insights into the annual dynamics of unexplored *Skeletonema* species; interestingly, species-specific annual dynamics were synchronized even in complex coastal waters with river inputs and disturbances (Fig. 5), despite differences in seasonality and occurrence patterns (Fig. 5) and their similar optimal temperatures according to a previous *ex situ* incubation experiment (Kaeriyama et al. 2011). This discrepancy indicates that other environmental variables control/co-control *Skeletonema* dynamics in natural waters. Biological endogenous rhythmicity could be a possible reason, as bloom dynamics were less variable compared with the highly variable environmental fluctuations (e.g. light insolation and nutrient concentration; Fig. 5 vs. Figs. 2 & 3) (Longobardi et al. 2022).

4.2. Seasonality

To discuss the seasonality of the target species, we defined summer and winter species based on the maximum copy numbers for April–September and October–March, respectively. The target *Skeletonema* species had different seasonality: 3 were summer species and 4 were winter species (Fig. 7). Although summer species showed positive growth rates in batch cultures even at <10°C (Kaeriyama et al. 2011, Li et al. 2021), they grow at higher temperatures (12.1°C–30.3°C) in coastal waters. In contrast, winter species increased their copy number at temperatures lower than their optimal (~25°C; Kaeriyama et al. 2011, Shevchenko et al. 2019) in the natural coastal waters of Ariake Sound. These different growth responses suggest that parameters other than temperature control their ecological success *in situ.* The different seasonality of the 7 *Skeletonema* species indicates differences in their physiology and ecological succession in natural environments. The species-specific seasonality observed in this study is consistent with another temporal monitoring report which mainly targeted *Skeletonema* using 28S rRNA amplicon sequencing (Canesi & Ryanearson 2016).

4.3. Occurrence patterns

The occurrence patterns were briefly categorized into 2 groups: (1) intense increase within a single peak and (2) moderate sustained increase with spiky variations (Fig. 7). The different patterns indicate different ecological strategies for each *Skeletonema* species. The single-peak species exhibited peak increases at different time points (Fig. 5D–F), suggesting that these species are 'short-stay visitors' that undergo an explosive increase under optimal environmental conditions, suddenly decreasing their numbers after the bloom. Their opportunistic proliferation under temporarily advantageous conditions is ecologically identical to those of copiotrophic

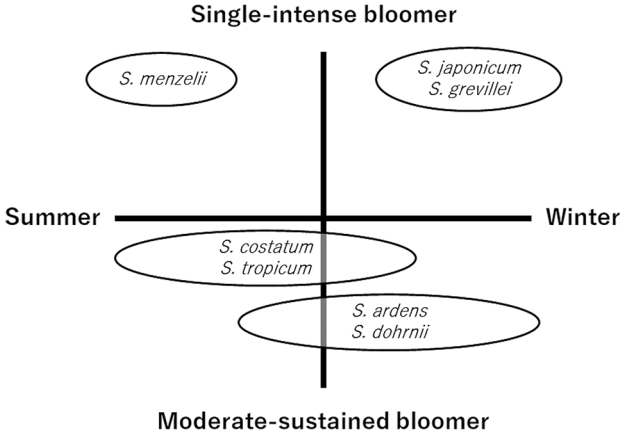

Fig. 7. Seasonal dynamics and occurrence patterns of each *Skeletonema* species

insects and bacteria (Pianka 1970, Kirchman 2012). Thus, these *Skeletonema* species might employ a survival strategy based on a single outburst. Alternatively, the multiple-peaked species sustained their copy number for a prolonged period, accompanied by frequent up-and-down variations (Fig. 5A–C,G). Interestingly, the copy numbers of these species generally overlapped. It has been postulated that 'long-lived tenants' gradually increase in number in a mixed assemblage (MacArthur 1972, Odum 1983, Kirchman 2012).

4.4. Environmental control: summer species

The summer environment in Ariake Sound is highly dynamic, similar to that observed with moderate and extreme freshening events (Fig. 2A,D). The river input of low-salinity water concurrently prompted a temporary stratification of the water column, as shown by the large E' values (Fig. 2B,E); this also provides nutrients to the surface water (i.e. negative relationships between nutrients and SSS; Fig. 3, Table 2). In addition, solar insolation and euphotic zone depth increase during the summer, improving light penetration into the water (Fig. 3) and positive relationships between Zeu and SSS (Table 2). This indicates a short-term stable and nutrient-replete environment after rainfall, potentially leading to an increase in the number of summer pioneer species (i.e. *S. menzelii*). However, *S. menzelii* was not detected in the summer of 2019 at Stn 355, although its copy number was significant in 2020 (Fig. 5F). It has been reported that *Skeletonema* species form resting cells in sediments (Hargraves 1976, Sakshaug & Andresen 1986, McQuoid & Hobson 1996); thus, resuspension of resting cells might be another factor driving the dynamics.

On the other hand, the long-lived tenants in summer, *S. costatum* and *S. tropicum*, responded to different environmental variables (Fig. 6, Table 3). The RDA outputs suggest that increased temperature might be critical for the onset of *S. costatum* (Fig. 6). This is similar to laboratory incubation and amplicon sequence results, which demonstrated enhanced growth of *S. costatum* at higher temperatures and in summer (Kaeriyama et al. 2011, Canesi & Ryanearson 2016). In general, summer species correlated with various environmental variables (Fig. 6). This notion could be supported by highly dynamic summer conditions with high river freshwater input and anticyclonic tropical typhoons; summer species might bloom when the environment is optimal for the growth of each species. In addition, biological endogenous rhythms (e.g. photoperiodic control) could partly drive the dynamics of these summer species (Lambert et al. 2019, Longobardi et al. 2022), as evidenced by some blooms which lasted several months even under highly dynamic environmental changes (Fig. 5).

4.5. Environmental control: winter species

The winter species also showed contrasting annual dynamics. The copy number of *S. ardens* was not related to SST; however, this species might favor low-light conditions like *S. dohrnii/marinoi* (Table 3). Low temperatures and solar insolation were observed in winter (Fig. 2A,C,D,F). Despite the difficulty of evaluating the temperature threshold for winter species from our data set, their maximum copy numbers were observed at 10–15°C (Figs. 2A & 5); this was associated with reduced solar insolation (Fig. 2C,F). Notably, as with summer species, the resuspension of resting cells in sediments affects the dynamics of surface water populations, particularly *S. ardens* and *S. dohrnii/marinoi,* showing multiple spikes throughout the winter (Fig. 5A,C). Interestingly, the installation of seaweed culturing structures excavates sediment in September/October, which may also significantly resuspend this sediment (Oohusa 1993, Kito & Kawamura 1999), particularly for *S. ardens* and *S. tropicum* (Fig. 5A,G).

As discussed above, *Skeletonema* form resting cells in sediments. Itakura et al. (1997) and Yamada et al. (2014) observed abundant viable dormant *Skeletonema* cells in the sediments of Japanese coastal waters (10^4–10^6 cells g sediment^{-1}). Japanese coastal waters are often disturbed by tropical typhoons in the summer, which can resuspend a considerable amount of sediment to the water column. During the winter, resuspension of the sediments can be caused by increased winter vertical mixing and seaweed culturing activities (e.g. installation of seaweed culturing structures). Thus, quantifying the amount and supply rate of resting cells is required to achieve a comprehensive understanding of annual *Skeletonema* dynamics in the future. Moreover, like summer species, resuspended dormant cells could simply be responding to their biological endogenous cycles (e.g. stimulated by the short photoperiod and/or intermittent light exposure with strong vertical mixing) (Lavaud et al. 2007, Malviya et al. 2016, Longobardi et al. 2022).

5. CONCLUDING REMARKS

Overall, the target *Skeletonema* species have specific seasonality and occurrence patterns (Fig. 5): there were summer and winter species, short-stay 'visitors' and long-lived 'tenants' (Fig. 7). Kooistra et al. (2008) and Kaeriyama et al. (2011) demonstrated the distributions and *ex situ* physiology in detailed studies. Our study was the first to investigate *in situ* species succession and annual dynamics using a novel qPCR technique. Our *in situ* species-specific monitoring study connects *ex situ* physiology with *in situ* distributions. In doing this, this study has revealed diverse ecophysiology within an important cosmopolitan diatom genus.

However, this study also has several limitations. First, zooplankton grazing and viral infections were not considered in this study; our qPCR results only reflect the abundance of *Skeletonema*. Further studies are needed to characterize zooplankton and viruses in Ariake Sound. Second, our pilot qPCR study was based on single-year results; thus, our species-specific ecological categorization needs to be further validated by multi-year observations. Third, we developed a species-specific qPCR technique targeting the 28S rRNA gene. However, our primer sets could not discriminate between *S. dohrnii* and *S. marinoi*; thus, primers designed within the 28S rRNA gene have limited applications to other *Skeletonema* species. In the future, other gene regions should be examined to discriminate *Skeletonema* species in global *Skeletonema* research. Given the scarcity of known *Skeletonema* genomes, it is difficult to find a suitable marker gene. Hence, high-quality *Skeletonema* genome sequences are needed for future research on this diatom genus.

Data availability. The data that support the findings of this study are available at: http://doi.org/10.34551/00023065.

Acknowledgements. This work was supported by 'Cooperating Monitoring Project in Ariake Sea' and 'Projects for Sophistication of Production and Utilization Technology Supporting Local Agriculture and Marine Industry'. This work was partly supported by JSPS KAKENHI Grant number 20H03327.

LITERATURE CITED

Anderson D, Hoagland P, Kaoru Y, White A (2000) Estimated annual economic impacts from harmful algal blooms (HABs) in the United States. Woods Hole Oceanographic Institution, Woods Hole, MA

Assmy P, Smetacek V, Montresor M, Ferrante MI (2019) Algal blooms. In: Schmidt TM (ed) Encyclopedia of microbiology, 4th edn. Academic Press, Cambridge, MA, p 61–79

Barton AD, Dutkiewicz S, Flierl G, Bragg J, Follows MJ (2010) Patterns of diversity in marine phytoplankton. Science 327:1509–1511

Behrenfeld MJ, Randerson JT, McClain CR, Feldman GC and others (2001) Biospheric primary production during an ENSO transition. Science 291:2594–2597

Bouman HA, Platt T, Doblin M, Figueiras FG and others (2018) Photosynthesis–irradiance parameters of marine phytoplankton: synthesis of a global data set. Earth Syst Sci Data 10:251–266

Canesi KL, Ryanearson TA (2016) Temporal variation of *Skeletonema* community composition from a long-term time series in Narragansett Bay identified using high-throughput DNA sequencing. Mar Ecol Prog Ser 556: 1–16

Cleve PT (1900) Notes on some Atlantic plankton-organisms. K Sven Vetensk Akad Handl 34:3–22

Cushing DH (1989) A difference in structure between ecosystems in strongly stratified waters and in those that are only weakly stratified. J Plankton Res 11:1–13

D'Silva MS, Anil AC, Naik RK, D'Costa PM (2012) Algal blooms: a perspective from the coasts of India. Nat Hazards 63:1225–1253

Day JW, Crump BC, Kemp WM, Yáñez-Arancibia A (2012) Estuarine ecology, 2nd edn. Wiley-Blackwell, Hoboken, NJ

de Vargas C, Audic S, Henry N, Decelle J and others (2015) Eukaryotic plankton diversity in the sunlit ocean. Science 348:1261605

Diaz RJ, Rosenberg R (2008) Spreading dead zones and consequences for marine ecosystems. Science 321: 926–929

Elder L, Elbrächter M (2010) The Utermöhl method for quantitative phytoplankton analysis. In: Karlson B, Cusack C, Bresnan E (eds) Microscopic and molecular methods for quantitative phytoplankton analysis. UNESCO, Paris, p 13–20

Endo H, Ogata H, Suzuki K (2018) Contrasting biogeography and diversity patterns between diatoms and haptophytes in the central Pacific Ocean. Sci Rep 8:10916

Enjoji N, Katano T, Yoshinaka Y, Furuoka F and others (2019) Development of primer sets for multiplex and qPCR assays targeting *Skeletonema* species and their application to field samples. J Oceanogr 75:319–334

Eriksen R, Trull TW, Davies D, Jansen P, Davidson AT, Westwood K, van den Enden R (2018) Seasonal succession of phytoplankton community structure from autonomous sampling at the Australian Southern Ocean Time Series (SOTS) observatory. Mar Ecol Prog Ser 589:13–31

Falkowski PG, Barber RT, Smetacek V (1998) Biogeochemical controls and feedbacks on ocean primary production. Science 281:200–206

Feng C, Ishizaka J, Saitoh K, Mine T, Yamashita H (2020) A novel method based on backscattering for discriminating summer blooms of the raphidophyte (*Chattonella* spp.) and the diatom (*Skeletonema* spp.) using MODIS images in Ariake Sea, Japan. Remote Sens 12:1504

Field CB, Behrenfeld MJ, Randerson JT, Falkowski P (1998) Primary production of the biosphere: integrating terrestrial and oceanic components. Science 281: 237–240

Guiry MD (2012) How many species of algae are there? J Phycol 48:1057–1063

Guo S, Sun J, Zhao Q, Feng Y, Huang D, Liu S (2016) Sinking rates of phytoplankton in the Changjiang (Yangtze River) estuary: a comparative study between *Prorocentrum dentatum* and *Skeletonema dorhnii* [sic] bloom. J Mar Syst 154:5–14

Hallegraeff GM, Jeffrey SW (1993) Annually recurrent diatom blooms in spring along the New South Wales coast of Australia. Aust J Mar Freshw Res 44:325–334

Hargraves PE (1976) Studies on marine plankton diatoms. II. Resting spore morphology. J Phycol 12:118–128

Hasle GR (1973) Morphology and taxonomy of *Skeletonema costatum* (Bacillariophyceae). Nor J Bot 20:109–137

Hasle GR, Syvertsen EE (1997) Marine diatoms. In: Tomas CR (ed) Identifying marine phytoplankton. Academic Press, London, p 5–386

Hydes DJ, Aoyama M, Aminot A, Bekker K and others (2010) Determination of dissolved nutrients (N, P, Si) in seawater with high precision and inter-comparability using gas-segmented continuous flow analysers. In: Hood EM, Sabine CL, Sloyan BM (eds) The GO-SHIP repeat hydrography manual: a collection of expert reports and guidelines. IOCCP Rep 14. ICPO Publ Ser 134. UNESCO-IOC, Paris. https://www.go-ship.org/HydroMan.html

Imai I, Itakura S, Matsuyama Y, Yamaguchi M (1996) Selenium requirement for growth of a novel red tide flagellate *Chattonella verruculosa* (Raphidophyceae) in culture. Fish Sci 62:834–835

Imai I, Yamaguchi M, Hori Y (2006) Eutrophication and occurrences of harmful algal blooms in the Seto Inland Sea, Japan. Plankton Benthos Res 1:71–84

Ishizaka J, Kitaura Y, Touke Y, Sasaki H and others (2006) Satellite detection of red tide in Ariake Sound, 1998–2001. J Oceanogr 62:37–45

Itakura S, Imai I, Itoh K (1997) 'Seed bank' of coastal planktonic diatoms in bottom sediments of Hiroshima Bay, Seto Inland Sea, Japan. Mar Biol 128:497–508

Kaeriyama H, Katsuki E, Otsubo M, Yamada M, Ichimi K, Tada K, Harrison PJ (2011) Effects of temperature and irradiance on growth of strains belonging to seven *Skeletonema* species isolated from Dokai Bay, southern Japan. Eur J Phycol 46:113–124

Kirchman DN (2012) Processes in microbial ecology. Oxford University Press, Oxford

Kirk JO (2010) Light and photosynthesis in aquatic ecosystems, 3rd edn. Cambridge University Press, Cambridge

Kito H, Kawamura Y (1999) The cultivation of *Porphyra* (nori) in Japan. World Aquac 30:35–37

Kooistra WHCF, Sarno D, Balzano S, Gu H, Andersen RA, Zingone A (2008) Global diversity and biogeography of *Skeletonema* species (Bacillariophyta). Protist 159: 177–193

Lambert S, Tragin M, Lozano JC, Ghiglione JF, Vaulot D, Bouget FY, Galan PE (2019) Rhythmicity of coastal marine picoeukaryotes, bacteria and archaea despite irregular environmental perturbations. ISME J 13: 388–401

Lavaud J, Strzepek RF, Kroth PG (2007) Photoprotection capacity differs among diatoms: possible consequences on the spatial distribution of diatoms related to fluctuations in the underwater light climate. Limnol Oceanogr 52:1188–1194

Legendre P, Gallagher ED (2001) Ecologically meaningful transformations for ordination of species data. Oecologia 129:271–280

Li H, Xu T, Ma J, Li F, Xu J (2021) Physiological responses of *Skeletonema costatum* to the interactions of seawater acidification and combination of photoperiod and temperature. Biogeosciences 18:1439–1449

Longobardi L, Dubroca L, Margiotta F, Sarno D, Zingone A (2022) Photoperiod-driven rhythms reveal multi-decadal stability of phytoplankton communities in a highly fluctuating coastal environment. Sci Rep 12:3908

Lucas LV, Cloern JE, Thompson JK, Stacey MT, Koseff JR (2016) Bivalve grazing can shape phytoplankton communities. Front Mar Sci 3:14

MacArthur RH (1972) Geographical ecology: patterns in the distribution of species. Harper & Row, New York, NY

Malviya S, Scalco E, Audic S, Vincent F and others (2016) Insights into global diatom distribution and diversity in the world's ocean. Proc Natl Acad Sci USA 113: E1516–E1525

McMinn A, Hallegraeff GM, Thomson P, Jenkinson AV, Heijnis H (1997) Cyst and radionucleotide evidence for the recent introduction of the toxic dinoflagellate *Gymnodinium catenatum* into Tasmanian waters. Mar Ecol Prog Ser 161:165–172

McMinn A, Ashworth C, Bhagooli R, Martin A, Salleh S, Ralph P, Ryan K (2012) Antarctic coastal microalgal primary production and photosynthesis. Mar Biol 159: 2827–2837

McQuoid MR, Hobson LA (1996) Diatom resting stages. J Phycol 32:889–902

Medlin LK, Elwood HJ, Stickel S, Sogin ML (1991) Morphological and genetic variation within the diatom *Skeletonema costatum* (Bacillariophyta): evidence for a new species, *Skeletonema pseudocostatum.* J Phycol 27: 514–524

Mino Y, Sukigara C, Honda MC, Kawakami H and others (2020) Seasonal and interannual variations in nitrogen availability and particle export in the northwestern North Pacific Subtropical Gyre. J Geophys Res Oceans 125:e2019JC015600

Murray G (1897) On the reproduction of some marine diatoms. Proc R Soc Edinb 21:207–219

Nelson DM, Tréguer P, Brzezinski MA, Leynaert A, Quéguiner B (1995) Production and dissolution of biogenic silica in the ocean: revised global estimates, comparison with regional data and relationship to biogenic sedimentation. Global Biogeochem Cycles 9:359–372

Odum EP (1983) Basic ecology. Saunders College Publishing, Philadelphia, PA

Ogura A, Akizuki Y, Imoda H, Mineta K, Gojobori T, Nagai S (2018) Comparative genome and transcriptome analysis of diatom, *Skeletonema costatum*, reveals evolution of genes for harmful algal bloom. BMC Genomics 19:765

Omura T, Iwataki M, Borja VM, Takayama H, Fukuyo Y (2012) Marine phytoplankton of the Western Pacific. Kōseishakōseikaku, Tokyo

Oohusa T (1993) The cultivation of *Porphyra* 'nori'. In: Ohno M, Critchley AT (eds) Seaweed cultivation and marine ranching. Japan International Cooperation Agency, Yokosuka, p 57–73

Orita R, Umehara A, Komorita T, Choi JW, Montani S, Komatsu T, Tsutsumi H (2015) Contribution of the development of the stratification of water to the expansion of dead zone: a sedimentological approach. Estuar Coast Shelf Sci 164:204–213

Orsini L, Sarno D, Procaccini G, Poletti R, Dahlmann J, Montresor M (2002) Toxic *Pseudo-nitzschia multi-*

striata (Bacillariophyceae) from the Gulf of Naples: morphology, toxin analysis and phylogenetic relationships with other *Pseudo-nitzschia* species. Eur J Phycol 37:247–257

Paasche E, Johansson S, Evensen DL (1975) An effect of osmotic pressure on the valve morphology of the diatom *Skeletonema subsalsum*. Phycologia 14: 205–211

Paerl HW, Justić D (2012) Estuarine phytoplankton. In: Day JW, Crump BC, Kemp WM, Yáñez-Arancibia A (eds) Estuarine ecology, 2nd edn. Wiley-Blackwell, Hoboken, NJ, p 85–110

Parsons TR, Maita Y, Lalli CM (1984) A manual of chemical and biological methods for seawater analysis. Pergamon Press, Oxford

Pearson LA, D'Agostino PM, Neilan BA (2021) Recent developments in quantitative PCR for monitoring harmful marine microalgae. Harmful Algae 108:102096

Pernet F, Malet N, Pastoureaud A, Vaquer A, Quéré C, Dubroca L (2012) Marine diatoms sustain growth of bivalves in a Mediterranean lagoon. J Sea Res 68: 20–32

Peterson BJ (1999) Stable isotopes as tracers of organic matter input and transfer in benthic food webs: a review. Acta Oecol 20:479–487

Pianka ER (1970) On *r*- and *K*-selection. Am Nat 104: 592–597

Poole HH, Atkins WRG (1929) Photo-electric measurements of submarine illumination throughout the year. J Mar Biol Assoc UK 16:297–324

Richardson K (1997) Harmful or exceptional phytoplankton blooms in the marine ecosystem. Adv Mar Biol 31: 301–385

Riley GA (1947) A theoretical analysis of zooplankton population of Georges Bank. J Mar Res 6:104–113

Rimet F, Gusev E, Kahlert M, Kelly MG and others (2019) Diat.barcode, an open-access curated barcode library for diatoms. Sci Rep 9:15116

Sakshaug E, Andresen K (1986) Effect of light regime upon growth rate and chemical composition of a clone of *Skeletonema costatum* from the Trondheimfjord, Norway. J Plankton Res 8:619–637

Sakshaug E, Bricaud A, Dandonneau Y, Falkowski PG and others (1997) Parameters of photosynthesis: definitions, theory and interpretation of results. J Plankton Res 19: 1637–1670

Sarmiento JL, Gruber N (2006) Ocean biogeochemical cycles. Princeton University Press, Princeton, NJ

Sarno D, Kooistra WHCF, Medlin LK, Percopo I, Zingone A (2005) Diversity in the genus *Skeletonema* (Bacillariophyceae). II. An assessment of the taxonomy of *S. costatum*-like species with the description of four new species. J Phycol 41:151–176

Sarno D, Kooistra WHCF, Balzano S, Hargraves PE, Zingone A (2007) Diversity in the genus *Skeletonema* (Bacillariophyceae): III. Phylogenetic position and morphological variability of *Skeletonema costatum* and *Skeletonema grevillei*, with the description of *Skeletonema ardens* sp. nov. J Phycol 43:156–170

Shevchenko OG, Ponomareva AA (2015) The morphology and ecology of the marine diatom *Skeletonema marinoi* Sarno et Zingone, 2005 from the Sea of Japan. Russ J Mar Biol 41:490–494

Shevchenko OG, Ponomareva AA, Turanov SV, Dutova DI (2019) Morphological and genetic variability of *Skeletonema dohrnii* and *Skeletonema japonicum* (Bacillariophyta) from the northwestern Sea of Japan. Phycologia 58:95–107

Shikata T, Nukata A, Yoshikawa S, Matsubara T and others (2009) Effects of light quality on initiation and development of meroplanktonic diatom blooms in a eutrophic shallow sea. Mar Biol 156:875–889

Smayda TJ (1973) The growth of *Skeletonema costatum* during a winter–spring bloom in Narragansett Bay, Rhode Island. J Bot 20:219–247

Suzuki T, Higgins PJ, Crawford DR (2000) Control selection for RNA quantitation. Biotechniques 29:332–337

Sverdrup HU, Johnson MW, Flemimg RH (1942) The oceans, their physics, chemistry, and general biology. Prentice-Hall, Inc., Englewood Cliffs, NJ

Tam J, Taylor MH, Blaskovic V, Espinoza P and others (2008) Trophic modeling of the Northern Humboldt Current Ecosystem, I. Comparing trophic linkages under La Niña and El Niño conditions. Prog Oceanogr 79:352–365

Thangaraj S, Sun J (2021) Transcriptomic reprogramming of the oceanic diatom *Skeletonema dohrnii* under warming ocean and acidification. Environ Microbiol 23: 980–995

Tomas CR (1997) Identifying marine phytoplankton. Academic Press, London

Tsutsumi H (2006) Critical events in the Ariake Bay ecosystem: clam population collapse, red tides, and hypoxic bottom water. Plankton Benthos Res 1:3–25

Vasselon V, Bouchez A, Rimet F, Jacquet S and others (2018) Avoiding quantification bias in metabarcoding: application of a cell biovolume correction factor in diatom molecular biomonitoring. Methods Ecol Evol 9: 1060–1069

Wang H, Chen F, Liu Q, Yu Z, Zhen Y (2020) Responses of marine diatom *Skeletonema marinoi* to nutrient deficiency: programmed cell death. Appl Environ Microbiol 86:1–16

Westwood KJ, Thomson PG, van den Enden RL, Maher LE, Wright SW, Davidson AT (2018) Ocean acidification impacts primary and bacterial production in Antarctic coastal waters during austral summer. J Exp Mar Biol Ecol 498:46–60

Wilson JR, Wilkerson FP, Blaser SB, Nielsen KJ (2021) Phytoplankton community structure in a seasonal low-inflow estuary adjacent to coastal upwelling (Drakes Estero, CA, USA). Estuaries Coasts 44:769–787

Yamada M, Otsubo M, Tsutsumi Y, Mizota Y and others (2013) Species diversity of the marine diatom genus *Skeletonema* in Japanese brackish water areas. Fish Sci 79:923–934

Yamada M, Otsubo M, Kodama M, Yamamoto K and others (2014) Species composition of *Skeletonema* (Bacillariophyceae) in planktonic and resting-stage cells in Osaka and Tokyo Bays. Plankt Benthos Res 9: 168–175

Yamaguchi A, Ota H, Mine T (2019) Growth environment of diatoms in turbid water in the inner western part of Ariake Bay during winter. J Oceanogr 75:463–473

Yoshida K, Endo H, Lawrenz E, Isada T, Hooker SB, Prášil O, Suzuki K (2018) Community composition and photophysiology of phytoplankton assemblages in coastal Oyashio waters of the western North Pacific during early spring. Estuar Coast Shelf Sci 212: 80–94

Yoshida K, Nakamura S, Nishioka J, Hooker SB, Suzuki K (2020) Community composition and photosynthetic physiology of phytoplankton in the western subarctic Pacific near the Kuril Islands with special reference to iron availability. J Geophys Res Biogeosciences 125:e2019JG005525

Zhang Q, Chen Z, Zhao J, Yu R and others (2020) Development of a sensitive qPCR method for the detection of pelagophyte *Aureococcus anophagefferens.* Limnol Oceanogr Methods 18:41–51

Zingone A, Percopo I, Sims PA, Sarno D (2005) Diversity in the genus *Skeletonema* (Bacillariophyceae). I. A reexamination of the type material of *S. costatum* with the description of *S. grevillei* sp. nov. J Phycol 41: 140–150

Editorial responsibility: Toshi Nagata, Kashiwanoha, Japan,
Reviewed by: 2 anonymous referees

Submitted: September 14, 2021
Accepted: October 21, 2022
Proofs received from author(s): December 8, 2022